Second-order John-Teller distortion in the thermally stable Li(La, Gd) MgWO$_6$:Eu^{3+} phosphor with high quantum efficiency

Quan Liu[a,b], Xibing Li[a,b], Jinkun Guo[c], Lixi Wang[a,b], Jangkun Song[c], Qitu Zhang[a,b,*]

[a] College of Materials Science and Engineering, Nanjing Tech University, Nanjing, 210009, China
[b] Jiangsu Collaborative Innovation Center for Advanced Inorganic Function Composites, Nanjing, 210009, China
[c] School of Electronic & Electrical Engineering, Sungkyunkwan University, Jangan-Gu, Suwon, Gyeonggi-do, 440-746, Republic of Korea

ARTICLE INFO

ABSTRACT

Thermally stable Li(La, Gd)MgWO$_6$:Eu^{3+} phosphors with high quantum efficiency were obtained by the sol-gel method. The symmetry of this double perovskite was reduced by doping Gd^{3+} ions in order to enhance the luminescence properties. In addition, phase structure and luminescence properties were characterized. A second-order John-Teller (SOJT) distortion of WO$_6$ octahedron existed in this double perovskite and was investigated in detail for the first time. The WO$_6$ octahedron of LiLa$_{0.95-x}$Gd$_x$Eu$_{0.05}$MgWO$_6$ distorted gradually and the SOJT distortion started to disappear while $x \geq 0.7$. Intensities of $^5D_0$-$^7F_2$ transition were greatly enhanced and reached the maximum at $x = 0.5$ under the excitation of 465 nm. The LiLa$_{0.45}$Gd$_{0.5}$Eu$_{0.05}$MgWO$_6$ phosphor showed excellent thermal stability and the thermal quenching mechanism was discussed by the configurational co-ordinate diagram. The optimized LiGd$_{0.5}$Eu$_{0.5}$MgWO$_6$ showed high quantum efficiency, which is much higher than commercial Y$_2$O$_2$S:Eu^{3+} and Y$_2$O$_3$:Eu^{3+} phosphors. The synthesized phosphors emit intense red light under the near ultraviolet and have great potential in light emitting diode.

1. Introduction

White light emitting diodes (LEDs) have kept booming in recent years and have been applied in many fields due to the advantages of energy saving and environmental protection [1–5]. Currently, commercial white LEDs combining ablue LED chip with yellow phosphors are being widely used. But this strategy lacks of red light and shows poor color rendering index, making it nonideal for indoor illumination [6–8]. Another way to get white light is combining a near ultraviolet (NUV) LED chip with tricolor phosphors. However, the luminescence intensity of red phosphors is much lower than that of green and blue phosphors [9,10]. And then the mixed white light deviates from natural white light. Therefore, red phosphors with high quantum efficiency, such as tungstate [11,12]/molybdate [13,14], titanate [15,16], vanadate [17,18] and phosphate [19,20], are in urgent needed to make up for red emission and improve the efficiency of UV LED.

Recently, molybdate and tungstate have been widely used because of their broad and strong charge transfer band (CTB) [5,21,22]. Typically, the double perovskite oxides with the formula A$_2$BMO$_6$ (A = Ba; B = Ca, Mg, Zn; M = W, Mo) attracted much more attention during the past years [23,24]. However, the quenching concentration of the active ions is low and the symmetry of this double perovskite is high, which is

not good for the red emission. In our previous work, "A$^+$ + A^{3+}" mode was selected to substitute "2 A^{2+}" mode and (Ka, Na, Li)LaMg-WO$_6$:Eu^{3+} phosphors were successfully synthesized [25–27]. The structure of NaLaMgWO$_6$ shows particular double order, layered or-dering of the A-site ions and rock-salt ordering of the B-site ions. Be-sides, the second-order John-Teller (SOJT) distortion of B'-site cations exists in this double perovskite. AA'BB'O$_6$ double perovskite has been proved to be an excellent matrix due to the high quenching con-centration. Of all these phosphors LiLaMgWO$_6$ has the lowest symmetry and LiLaMgWO$_6$:Eu^{3+} shows the best luminescence properties. As known, the symmetry of the double perovskite is related to the toler-ance factor. In order to reduce the symmetry of the double perovskite, ions with smaller radius were selected to substitute A-site ions of the double perovskite and the properties of the phosphors were greatly enhanced. Based on above ideas, Gd^{3+} ions were selected to substitute La^{3+} ions of LiLaMgWO$_6$ to reduce the tolerance factor and further reduce the symmetry. Continuing doping ions with smaller radius, the BO$_6$ octahedron would keep reversing. The SOJT distortion of Li-LaMgWO$_6$ was investigated in detail. Optimized double perovskite phosphor was compared with the commercial phosphors and the phosphors reported.

---

2. Experimental

The phosphors synthesized by the sol-gel method show high homogeneity and purity. Besides, the powders can be synthesized at lower temperature compared with the traditional solid-state reaction method. In this paper, all power samples were obtained by the sol-gel method. $LiNO_3$ (AR), La_2O_3 (99.99%), $Mg(NO_3)_2$ (AR), $(NH_4)_{10}W_{12}O_{41}$ (AR), Eu_2O_3 (99.99%), Gd_2O_3 (99.99%), HNO_3 (AR), $NH_3 \cdot H_2O$ (AR), citric acid (AR) and polyethylene glycol (PEG) were used as the starting materials. Rare earth oxides were dissolved in HNO_3 to prepare nitrate. Stoichiometric nitrates were added into deionized water and mixed by magnetic stirrer for 10 min. PEG and citric were added into the nitrate solution and mixed. $(NH_4)_{10}W_{12}O_{41}$ was dissolved in deionized water and the pH value of the solution was modulated to 6.0–8.0. All the solutions were mixed and heated to 80–90 °C. Then the solution was stirred until the transparent gel appeared. After then, the gel was moved to the oven with the temperature of 200 °C to get the fluffy precursor. Finally, the precursor was calcined at 1100 °C for 6 h and series of $LiLa_{0.95-x}Gd_xMgWO_6:Eu^{3+}$ (x = 0, 0.1, 0.3, 0.5, 0.7, 0.95) powders were obtained.

The crystalline phases were determined by X-ray diffraction (XRD, smartlabTM 9 kW, Rigaku, Japan) using Cu Kα radiation. The powders were tested in the range of 5–80° with a scanning rate of 5°/min and a step size 0.02°. Structure refinements were performed by the GSAS software and the crystal structure was obtained by Diamond. Morphologies of the samples were observed by transmission electron microscopy (TEM, FEI G2F20). Excitation and emission spectra were measured by the fluorescent spectrophotometer (Lumina, America). A heating furnace was used while testing the thermal performance of the phosphor. The quantum yields (QYs) were performed by an external integrating sphere coupled with the spectrofluorometer by optical fibers. The luminous efficiency (LE), correlated color temperature (CCT), and color rendering index (CRI) of the fabricated WLED devices were evaluated using an integrating sphere.

3. Results and discussion

The XRD patterns of $LiLa_{0.95-x}Gd_xMgWO_6$ are shown in Fig. 1. The patterns matched well with the double perovskite structure of $NaLaMgWO_6$ (JCPDS #88–1761). The 2θ of ~11° and ~25° indicated that layered ordering of the A-site cations existed in this system. In addition, the supperlattice diffraction peak at ~19.0° and ~38.0° belonged to the rock salt ordering of MgO_6 and WO_6 octahedrons [28]. Layered ordering of A-site cations and the SOJT distortion of B' cations co-existed in this double perovskite [29,30]. The structure of double perovskite existed stably when x ≤ 0.5 and impurity phase turned up when x ≥ 0.7. Therefore, SOJT distortion of B' cations gradually vanished when x ≥ 0.7. Tolerance factors (t) of $LiLa_{0.95-x}Gd_xEu_{0.05}MgWO_6$, deciding the crystal structure of double perovskite, are shown in Table 1. With increasing Gd^{3+} concentration with smaller ionic radius, tolerance factor gradually decreased from 0.868 to 0.830. Obviously, SOJT distortion of B' cations existed stably when t ≥ 0.847 and started to disappear while t ≤ 0.839.

$$t = \frac{r_{Li} + 0.05r_{Eu} + (0.95 - x)r_{La} + xr_{Gd} + 2r_O}{\sqrt{2(r_{Mg} = +r_W + 2r_O)}} \qquad (1)$$

Structure information was obtained by Rietveld refinements and the results were shown in Table 2. As reported, the $LiLaMgWO_6$ belongs to a monoclinic system with the space group of $C2/m$ ($a^0b^-c^0$). Therefore, the space group of $C2/m$ was selected as the starting model. The cell parameters are a = 7.808 Å, b = 7.811 Å, c = 7.886 Å, and V = 480.94 Å³ for $LiLa_{0.95}Eu_{0.05}MgWO_6$ and a = 7.699 Å, b = 7.771 Å, c = 7.807 Å, and V = 467.04 Å³ for $LiLa_{0.45}Gd_{0.5}Eu_{0.05}MgWO_6$, respectively. The Rietveld refinement of the observed XRD patterns and the crystal structure of $LiLa_{0.45}Gd_{0.5}Eu_{0.05}MgWO_6$ are shown in Fig. 2.
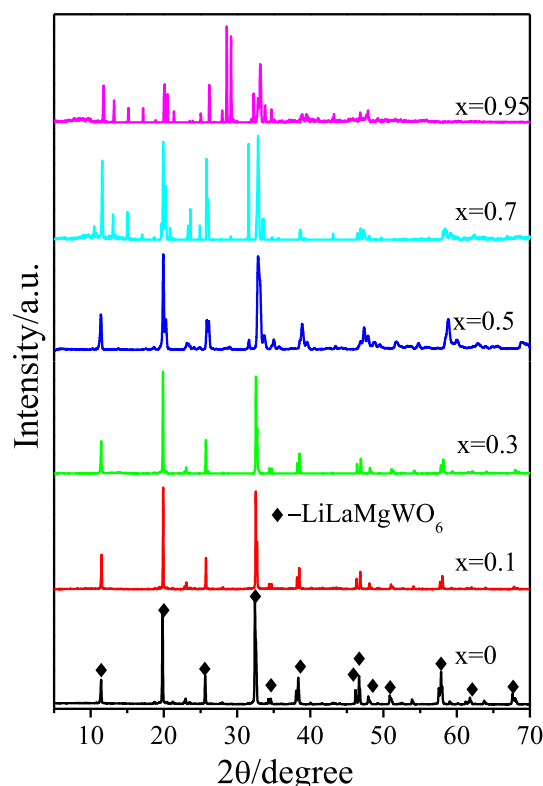

Fig. 1. XRD pattern of $LiLa_{0.95-x}Gd_xEu_{0.05}MgWO_6$ (x = 0, 0.1, 0.3, 0.5, 0.7, 0.95).

Table 1
Tolerance factors of $LiLa_{0.95-x}Gd_xEu_{0.05}MgWO_6$.

x	0	0.1	0.3	0.5	0.7	0.95
t	0.868	0.864	0.856	0.847	0.839	0.830

Table 2
Cell parameters of $LiLa_{0.95}Eu_{0.05}MgWO_6$ and $LiLa_{0.45}Gd_{0.5}Eu_{0.05}MgWO_6$ obtained from Rietveld refinement.

	$LiLa_{0.95}Eu_{0.05}MgWO_6$	$LiLa_{0.45}Gd_{0.5}Eu_{0.05}MgWO_6$
Space Group	C2/m	C2/m
a(Å)	7.808	7.699
b(Å)	7.811	7.771
c(Å)	7.886	7.807
V(Å³)	480.94	467.04
Ln-O$_{ave}$(Å)	2.564	2.458
W-O$_1$(Å)	1.903	1.894
W-O$_2$(Å)	1.916	1.895
W-O$_3$(Å)	1.821	1.813
W-O$_4$(Å)	1.980	1.960
W-O$_5$(Å)	2.142	2.134
Distortion($\Delta \times 10^5$)	263.6	267.6

The refine R-values were 10.44% (Rwp) and 6.43% (Rp). In the crystal structure of $LiLaMgWO_6$, Li^+ and La^{3+} coordinated with 12 O^{2-} ions to form polyhedral while Mg^{2+} and W^{6+} coordinated with 6 O^{2-} ions to form MgO_6 octahedron and WO_6 octahedron. The MgO_6 octahedron and WO_6 octahedron connected with each other by means of sharing the same site. Obviously, the structure showed layered ordering of A-site ions and rock-salt ordering of MgO_6 octahedron and WO_6 octahedron. Fig. 2 (e) shows the schematic illustration of the LaO_{12} octahedrons of $LiLa_{0.45}Gd_{0.5}Eu_{0.05}MgWO_6$. Fig. 2 (c) and Fig. 2 (d) give the schematic illustration of the WO_6 octahedrons of $LiLa_{0.95}Eu_{0.05}MgWO_6$ and $LiLa_{0.45}Gd_{0.5}Eu_{0.05}MgWO_6$, which show the SOJT distortion. As can